An essential GDP-Fuc: β-*D*-Gal α-1,2-fucosyltransferase is located in the mitochondrion of *Trypanosoma brucei*

Giulia Bandini[a,1,2], Sebastian Damerow[a,1,3], Maria Lucia Sampaio Güther[a], Angela Mehlert[a], Hongjie Guo[b], Stephen M. Beverley[b] and Michael A. J. Ferguson[a,4]

[a]Wellcome Centre for Anti-Infectives Research, School of Life Sciences, University of Dundee, Dundee, DD1 5EH, United Kingdom.

[b]Department of Molecular Microbiology, Washington University School of Medicine, St. Louis, MO 63110, USA.

[1]These authors contributed equally to this work.

[2]Current address: Department of Molecular and Cell Biology, Boston University Goldman School of Dental Medicine, Boston MA 02118, USA

[3]Current address: Richter-Helm BioLogics GmbH, Suhrenkamp 59, 22335 Hamburg, Germany

[4]Corresponding author. Mailing address: Wellcome Centre for Anti-Infectives Research, School of Life Sciences, University of Dundee, Dow St., Dundee DD1 5EH, Scotland, United Kingdom. Phone: 44-1382-384219. Fax: 44-1382-348896. E-mail: m.a.j.ferguson@dundee.ac.uk

Classification: Biological Sciences, Microbiology

Short title: Mitochondrial fucosyltransferase in *T. brucei*

Keywords: mitochondria, *Trypanosoma brucei*, glycobiology, glycosyltransferase, fucose

Author contributions: G.B., S.D., and M.A.J.F. designed research; G.B., S.D., M.L.S.G. and H.G. performed research; G.B., S.D., A. M., S.M.B., and M.A.J.F. analysed data; G.B., S.D., S.M.B. and M.A.J.F. wrote the paper.

ABSTRACT

The biosynthesis of guanosine 5′-diphospho-β-*L*-fucose (GDP-Fuc), the activated donor for fucose, has been shown to be essential in the parasite *Trypanosoma brucei*. Fucose is a common constituent of eukaryotic glycan structures, but it has been rarely found in trypanosomatid glycoconjugates. A single putative *T. brucei* fucosyltransferase (*TbFUT1*) gene was identified in the trypanosome genome. The encoded TbFUT1 protein was enzymatically active when expressed in *Escherichia coli*. Structural characterization of its reaction products identified it as a GDP-Fuc: β-D-galactose α-1,2-fucosyltransferase, with a preference for a Galβ1,3GlcNAcβ1-O-R acceptor motif among the substrates tested. Conditional null mutants of the *TbFUT1* gene demonstrated that it is essential for growth of the mammalian-infective bloodstream form and insect vector dwelling procyclic form of the parasite. Unexpectedly, TbFUT1 was localized in the mitochondrion of *T. brucei* and found to be essential for mitochondrial function in bloodstream form trypanosomes, suggesting this kinetoplastid parasite possesses an unprecedented and essential mitochondrial fucosyltransferase activity.

41 **SIGNIFICANCE**

42 The sugar fucose is a well-known component of cell-surface glycoproteins and glycolipids and
43 typically plays roles in cell-cell adhesion. Fucose is generally incorporated into glycoproteins and
44 glycolipids by fucosyltransferase enzymes that reside in the Golgi apparatus. Here we show that
45 the single fucosyltransferase of the protozoan parasite *Trypanosoma brucei*, causative agent of
46 human and animal African trypanosomiasis, resides in the mitochondrion and not the Golgi
47 apparatus. While the exact role of fucosylation in the parasite mitochondrion remains to be
48 determined, it is essential for mitochondrial function and for parasite growth and survival. The
49 unusual nature of this parasite enzyme, and its orthologues in related parasite pathogens, suggests
50 that selective inhibitors may have therapeutic potential across a family of parasites.

51

52 **INTRODUCTION**

53 The protozoan parasites of the *Trypanosoma brucei* group are the causative agents of
54 human and animal African trypanosomiasis. Bloodstream form *T. brucei* are ingested by the
55 tsetse fly vector and differentiates into the procyclic form parasites to colonize the tsetse midgut.
56 To infect a new mammalian host, *T. brucei* undergoes a series of differentiations that allows it to
57 colonize the salivary gland of the fly and to be transferred to a new host during a subsequent
58 blood meal (1).

59 The surface coat of the bloodstream form is characterized by the GPI-anchored, *N*-
60 glycosylated variant surface glycoprotein (VSG) (2–5), while procyclic cells express a family of
61 GPI-anchored proteins called procyclins (6–9), free glycoinositolphospholipids (10–12) and a
62 high molecular weight glycoconjugate complex (13). The importance of glycoproteins to parasite
63 survival and infectivity has led to the investigation of enzymes of GPI anchor (14–17) and
64 nucleotide sugar (18–24) biosynthesis as potential therapeutic targets.

65 Nucleotide sugars are used as glycosyl donors in many glycosylation reactions. GDP-
66 Fucose (GDP-Fuc) was identified in the nucleotide sugar pools of *T. brucei*, *Trypanosoma cruzi*
67 and *Leishmania major* (25) and its biosynthesis is essential for parasite growth in procyclic and
68 bloodstream form *T. brucei* (26) and in *L. major* promastigotes (27). Interestingly, *T. brucei* and
69 *L. major* use different pathways to synthesize GDP-Fuc. *T. brucei* utilizes the *de novo* pathway in
70 which GDP-Fuc is synthesised from GDP-Mannose via GDP-mannose-4,6-dehydratase (GMD)
71 and GDP-4-keto-6-deoxy-D-mannose epimerase/reductase (GMER) (25, 26). Conversely, *L.*
72 *major* has two related bifunctional arabino/fuco-kinase/pyrophosphorylases, AFKP80 and FKP40
73 that synthesise GDP-Fuc from free fucose (27). The only structurally-defined fucose-containing
74 oligosaccharide in trypanosomatids is the low-abundance Ser/Thr-phosphodiester-linked glycan
75 on *T. cruzi* gp72, a glycoprotein that has been implicated in flagellar attachment (28–30).

76 Fucosyltransferases (FUTs) catalyse the transfer of fucose from GDP-Fuc to glycan and
77 protein acceptors and are classified into two superfamilies (31, 32). One superfamily contains all
78 α1,3/α1,4-FUTs (Carbohydrate Active EnZyme, CAZy, family GT10) and the other contains all
79 α1,2-, α1,6- and protein *O*-fucosyltransferases (GT11, GT23, GT37, GT65 and GT68) (33). In
80 eukaryotes, the vast majority of fucosyltransferases are type II transmembrane Golgi proteins
81 (34), but two exceptions have been described: (i) PgtA, a cytoplasmic bifunctional β1,3-
82 galactosyltransferase / α1,2-FUT found in *Dictyostelium discoideum* and *Toxoplasma gondii* (35,
83 36) that is part of an oxygen-sensitive glycosylation pathway that attaches a pentasaccharide to
84 the Skp1-containing ubiquitin ligase complex (37); and (ii) SPINDLY, a protein *O*-
85 fucosyltransferase that modifies nuclear proteins in *Arabidopsis thaliana* and *T. gondii* (38, 39).
86 Unusually, *T. brucei* and other kinetoplastids contain a single mitochondrion. In the
87 bloodstream form of the parasite this organelle has a tubular structure, while in the procyclic form
88 it is organized in a complex network with numerous cristae, reflecting the absence and presence,
89 respectively, of oxidative phosphorylation (1, 40). The parasite mitochondrion is further
90 characterized by a disc-shaped DNA network called the kinetoplast (41) that is physically linked
91 with the flagellum basal body (42, 43).
92 While secretory pathway and nuclear/cytosolic glycosylation systems have been studied
93 extensively, little is known about glycosylation within mitochondria. A glycoproteomic approach
94 in yeast revealed several mitochondrial glycoproteins (44), but it was not determined whether
95 these were imported from secretory pathway or glycosylated within the mitochondria by as yet
96 unknown glycosyltransferases. The only characterized example of a mitochondrial
97 glycosyltransferase is the mitochondrial isoform of mammalian *O*-GlcNAc transferase (OGT). *O*-
98 GlcNAcylation is a cycling modification, involved in signalling, in which OGT adds GlcNAc to
99 Ser/Thr residues and *O*-GlcNAcase (OGA) removes it (45). Recent studies have shown that both

100 mitochondrial OGT (mOGT) and OGA are present and active in mammalian mitochondria and
101 putative mitochondrial targets have been identified (46, 47). Further, a mammalian mitochondrial
102 UDP-GlcNAc transporter associated with mitochondrial *O*-GlcNAcylation has been recently
103 described (46). However, orthologues of OGT and OGA genes are not present in kinetoplastids.

104 Here, we report on a gene (*TbFUT1*) encoding a mitochondrial α-1,2-fucosyltransferase
105 protein (TbFUT1) in *T. brucei* that is essential to parasite survival.

106

107 **RESULTS**

108 ***Identification, cloning and sequence analysis of TbFUT1.*** The CAZy database lists eight
109 distinct FUT families: GT10, 11, 23, 37, 56, 65, 68 and 74 (32). One or more sequences from
110 each family were selected for BLASTp searches of the predicted proteins from the *T. brucei, T.*
111 *cruzi* and *L. major* genomes (Table S1). Strikingly, only one putative *T. brucei* fucosyltransferase
112 gene (*TbFUT1*) was identified from the *T. brucei* genome (GeneDB ID: Tb927.9.3600) belonging
113 to the GT11 family, which is comprised almost exclusively of α-1,2-FUTs (31, 48). Homologues
114 of *TbFUT1* were also found in the *T. cruzi* and *L. major* genomes and, unlike *T. brucei*, *T. cruzi*
115 and *L. major* also encode for GT10 FUT genes (Table S1).

116 The TbFUT1 predicted amino acid sequence shows relatively low sequence identity to
117 previously characterized GT11 FUTs, for example to *H. pylori* (26%) or human FUT2 (21%) (49,
118 50). Nevertheless, conserved motifs characteristic of this family can be clearly identified (Fig.
119 S1*A*) (33, 51). Motif I (aa 153-159) is shared with α-1,6-FUTs and has been implicated in the
120 binding of GDP-Fuc (52), whereas no clear functions have yet been assigned to motifs II, III and
121 IV (aa 197-207, 265-273 and 13-18, respectively). Although TbFUT contains a possible
122 transmembrane (TM) domain at its N-terminus, as would be expected of a typical Golgi-localized
123 fucosyltransferase (34), this putative TM domain (residues 6-28) overlaps with the

124 fucosyltransferase motif IV, which normally occurs after the TM domain (Fig. S1*A*). Indeed,
125 further analysis of the TbFUT predicted amino acid sequence using *PSort II (53)*, *Target P* (54)
126 and *Mitoprot* (55) suggested mitochondrial localization and identified a putative mitochondrial
127 targeting motif (M/L..RR) with RR at sequence position +30, similar to those described for other
128 eukaryotes. Conservation of this targeting motif has been previously shown for other parasite
129 mitochondrial proteins (56, 57). Further BLASTp searches show that there is generally a single
130 TbFUT1 gene homologue in each kinetoplastid species, and a phylogram of FUT sequences
131 shows that TbFUT1 homologues form a distinct clade closest to bacterial α-1,2-
132 fucosyltransferases (Fig. S1*B*).
133
134 ***Recombinant expression of TbFUT1***. The *TbFUT1* ORF was amplified from *T. brucei* 427
135 genomic DNA and cloned in the pGEX6P1 expression vector. The resulting construct
136 (pGEX6P1-GST-PP-*TbFUT1*) encoded for the *TbFUT1* ORF with a glutathione-S-transferase
137 (GST) tag at its N-terminus and a PreScission™ Protease (PP) cleavage site between the two
138 protein-encoding sequences. Sequencing identified a few nucleotide and amino acid differences
139 between the 427 and 927 strains, all of which are consistent with the partial genome assembly of
140 strain 427 (58). The pGEX6P1-GST-PP-*TbFUT1* construct was expressed in *E. coli* and the
141 fusion protein purified as described in Methods and Methods SI. The identities of the two higher
142 molecular weight bands (Fig. S2, lane 8) were determined by peptide mass fingerprinting. The
143 most abundant band was identified as TbFUT1, while the fainter band was identified as a subunit
144 of the *E. coli* GroEL chaperonin complex. The apparent molecular weight of GST-PP-TbFUT1
145 chimeric protein (57 kDa) was consistent with the predicted theoretical molecular weight (58.1
146 kDa).
147

148 ***Recombinant TbFUT1 is active in vitro.*** The recombinantly expressed GST-TbFUT1 fusion
149 protein was tested for activity by incubation with GDP-[^{3}H]Fuc as a donor and a panel of
150 commercially available mono- to octasaccharides (Table 1) selected from the literature as
151 possible α-1,2-FUT substrates (48, 49, 51). The effectiveness of each acceptor was evaluated
152 based on the presence/absence and intensities of the TLC bands corresponding to the
153 radiolabelled reaction products (Fig. 1 and Table 1). GST-TbFUT1 showed its best activity with
154 Galβ1,3GlcNAc (LNB) (Fig. 1, lane 2 and 5) and its β-O-Methyl glycoside (Fig. 1, lane 23).
155 Other larger oligosaccharides containing Galβ1,3GlcNAcβ1-O-R as a terminal motif (LNT and
156 LNH) were also good acceptors (Fig. 1, lanes 13 and 16), with the exception of iLNO (Fig. 1,
157 lane 15). Lactose was also an acceptor (Fig. 1, lane 1), while LacNAc and the LacNAc-
158 terminating branched hexasaccharide LNnH were weak acceptors (Fig. 1, lanes 3 and 12).
159 Interestingly, TbFUT1 was also able to transfer fucose to 3'-fucosyllactose, albeit inefficiently
160 (Fig. 1, lane 18), whereas no transfer could be seen to Galβ1,6GlcNAc (Fig. 1, lane 17) or to free
161 Gal or β-Gal-O-methyl (Fig. 1, lanes 11 and 22). As expected, no products were observed when
162 acceptor oligosaccharides were omitted from the reaction (Fig. 1, lane 6). To confirm the detected
163 activities were specific to the recombinant GST-TbFUT1, and not due to some co-purifying
164 endogenous *E. coli* contaminant, the assay was also performed using material prepared from *E.*
165 *coli* expressing the empty pGEX6P1 vector. No transfer of radiolabelled fucose could be
166 observed in these cases (Fig. 1, lanes 7-9).

167 A band with the same mobility as free fucose was always present in the assay reactions
168 and was considerably stronger in the presence of the GST-TbFUT1 preparation (Fig. 1, lanes 1-6
169 and 11-24), than when GDP-[^{3}H]Fuc was incubated with the reaction buffer alone (Fig. 1, lane
170 10) or in the presence of the material purified from the *E. coli* cells transformed with the empty
171 vector (Fig. 1, lanes 7-9). These data suggest that TbFUT1 has a significant propensity to transfer

172 Fuc to water. Interestingly, one of the substrates (LNB-O-Me; Galβ1,3GlcNAcβ1-O-methyl)
173 suppressed the amount of free Fuc produced in the reaction (Fig. 1, lane 23), suggesting that this
174 sugar may bind more tightly to the TbFUT1 acceptor site than the other glycans and thus prevent
175 the transfer of Fuc from GDP-Fuc to water.

176 The inverting α-1,2 and α-1,6-FUTs are independent of divalent cations for their activity
177 (51, 59–61). To study the dependence of TbFUT1 on these co-factors, the assay was repeated in
178 buffer without divalent cations or containing EDTA. No change in activity was observed in either
179 case, indicating TbFUT1 does not require divalent cations for its activity (Fig. S3).

180

181 ***Characterization of the TbFUT1 reaction product.*** The glycan reaction products were
182 structurally characterized to determine the anomeric and stereochemical specificity of TbFUT1.
183 Initially, we performed exoglycosidase and/or acid treatment of the radiolabelled reaction
184 products (recovered by preparative TLC) utilizing Lac, LacNAc and LNB as substrates. The
185 tritium label ran with the same mobility as authentic Fuc after acid hydrolysis of all three
186 products (Fig. S4*A* and *C*) and after *Xanthomonas manihotis* α-1,2-fucosidase digestion of the
187 Lac and LNB products (Fig. S4*B* and *C*). These data suggest that [^{3}H]Fuc was transferred in α1,2
188 linkage to the acceptor disaccharides.

189 To obtain additional and definitive data, we performed a large-scale activity assay using
190 LNB-O-Me as an acceptor and purified the reaction product by normal phase HPLC. Fractions
191 containing the putative fucosylated trisaccharide product (Fig. S5) were pooled and analysed for
192 their neutral monosaccharide content, which showed the presence of Fuc, Gal and GlcNAc. The
193 purified reaction product was then permethylated and analysed by ESI-MS (Fig. 2*A*), which
194 confirmed that the main product was a trisaccharide of composition $dHex_1Hex_1HexNAc_1$. The
195 MS/MS spectrum was also consistent with the dHex residue being attached to the Hex, rather

196 than HexNAc, residue (Fig. 2*B*). Subsequently, partially methylated alditol acetates (PMAAs)
197 were generated from the purified trisaccharide product and analysed by GC-MS. This analysis
198 identified derivatives consistent with the presence of non-reducing terminal-Fuc, 2-*O*-substituted
199 Gal and 3-*O*-substituted GlcNAc (Fig. S6 and Table 2), consistent with Fuc being linked to the
200 position 2 of Gal. The GC-MS methylation linkage analysis also revealed a trace of 2-*O*-
201 substituted Fuc in the sample which, together with the observation that 3'-FL can act as a weak
202 substrate (Fig. 1, lane 18 and Table 1), may suggest that TbFUT1 can also form Fucα1,2Fuc
203 linkages.

204 The purified TbFUT1 reaction product was also exchanged into deuterated water (^2H_2O)
205 and analysed by one-dimensional ^{1}H-NMR and two-dimensional ^{1}H-ROESY (Rotating frame
206 Overhouser Effect SpectroscopY). The ^{1}H-NMR spectrum showed a doublet at about 5.1 ppm,
207 consistent with the signal from the proton on the anomeric carbon (H_1) of an α-Fuc residue (Fig.
208 3*A*). A characteristic doublet for the anomeric proton of a β-Gal residue was also observed at 4.5
209 ppm. In the ^{1}H-ROESY spectrum, a cross-peak (labelled *a*) could be observed indicating a
210 through-space connectivity between the H_1 of α-Fuc and the H_2 of a β-Gal, consistent with a
211 Fucα1,2Gal linkage in the TbFUT1 reaction product (Fig. 3*B*). The chemical shifts that could be
212 clearly assigned by either one-dimensional ^{1}H-NMR or two-dimensional ^{1}H-ROESY are listed in
213 (Table 3).

214 Taken together, these data unambiguously define the structure of the TbFUT1 reaction
215 product with GDP-Fuc and LNB-O-Me as Fucα1,2Galβ1,3GlcNAcβ1-O-CH_3 which, in turn,
216 defines TbFUT1 as having a GDP-Fuc : βGal α-1,2 fucosyltransferase activity with a preference
217 for a Galβ1,3GlcNAcβ1-O-R acceptor motif.

218

219 ***Generation of TbFUT1 conditional null mutants in procyclic and bloodstream form T. brucei.***
220 Semi-quantitative RT-PCR showed that *TbFUT1* mRNA was present in both bloodstream form
221 and procyclic form *T. brucei*. We therefore sought to explore TbFUT1 function in both lifecycle
222 stages by creating *TbFUT1* conditional null mutants. The strategies used to generate the mutants
223 are described in (Fig. 4). The creation of these mutants was possible because genome assembly
224 indicated *TbFUT1* to be present as a single copy per haploid genome, and Southern blot analysis
225 using a *TbFUT1* probe was consistent with this prediction (Fig. S7). In procyclic cells (Fig. 4, left
226 panel), the first *TbFUT1* allele was replaced by homologous recombination with linear DNA
227 containing the puromycin resistance gene (*PAC*) flanked by about 500 bp of the *TbFUT1* 5'- and
228 3'-UTRs. After selection with puromycin, an ectopic copy of *TbFUT1,* under the control of a
229 tetracycline-inducible promoter, was introduced in the ribosomal DNA (rDNA) locus using
230 phleomycin selection. Following induction with tetracycline, the second allele was replaced with
231 the *BSD* gene by homologous recombination, generating the final procyclic form
232 *ΔTbFUT1::PAC/TbFUT1*^{Ti}*/ΔTbFUT1::BSD* conditional null mutant cell line (PCF *TbFUT1*
233 cKO). In bloodstream form cells (Fig. 4, middle panel), an ectopic copy of *TbFUT1* carrying a C-
234 terminal MYC_3 epitope tag under the control of a tetracycline-inducible promoter was first
235 introduced into the ribosomal DNA (rDNA) locus using phleomycin selection. Following cloning
236 and induction with tetracycline, the first *TbFUT1* allele was then targeted for homologous
237 recombination with linear DNA containing the hygromycin resistance gene (*HYG*) flanked by
238 about 1200 bp of the *TbFUT1* 5'- and 3'-UTRs. After selection with hygromycin, Southern
239 blotting revealed that gene conversion had taken place and that both *TbFUT1* alleles had been
240 replaced by *HYG* yielding a bloodstream form *TbFUT1-*
241 *MYC*$_3^{Ti}$*/ΔTbFUT1::HYG/ΔTbFUT1::HYG* conditional null mutant cell line (BSF *TbFUT1*-MYC_3
242 cKO). Southern blotting data confirming the genotypes of these mutants are shown in Fig. S7.

243 The BSF cell line was also used to generate a *TbFUT1*^{Ti}/*ΔTbFUT1::HYG*/*ΔTbFUT1::HYG*
244 conditional null mutant cell line by *in situ* homologous recombination of the tetracycline
245 inducible *TbFUT1*-MYC$_3$ copy, converting it to an untagged *TbFUT1* gene and generating BSF
246 *TbFUT1* cKO (Fig. 4, right panel).
247
248 ***TbFUT1 is essential to procyclic and bloodstream form T. brucei.*** Procyclic and bloodstream
249 form *TbFUT1* conditional null mutants were grown under permissive (plus tetracycline) or non-
250 permissive (minus tetracycline) conditions. The PCF *TbFUT1* cKO cells grown under non-
251 permissive conditions showed a clear reduction in the rate of cell growth after 6 days, eventually
252 dying after 15 days (Fig. 5*A*). The BSF *TbFUT1* cKO cells grew like wild type cells under
253 permissive conditions, whether or not the expressed TbFUT1 had a C-terminal MYC$_3$ tag, and
254 under non-permissive conditions also showed a clear reduction in the rate of cell growth after 2-4
255 days, dying after 3-5 days (Fig. 5*B* and *C*). These growth phenotypes are very similar to those
256 described for procyclic and bloodstream form *TbGMD* conditional null mutants that cannot
257 synthesise GDP-Fuc under non-permissive conditions (Fig. S8) (26). This is consistent with the
258 hypothesis that TbFUT1 may be the only enzyme that utilizes GDP-Fuc, or at least that it is the
259 only FUT transferring fucose to essential acceptors. Further evidence that TbFUT1 is essential for
260 procyclic and bloodstream form growth was obtained from Northern blots (Fig. 5*D* and *E*). These
261 show that *TbFUT1* mRNA levels are undetectable for several days after the removal of
262 tetracycline, but that growth resumes only when some cells escape tetracycline control after about
263 29 days (procyclic form) and 11 days (bloodstream form). Escape from tetracycline control after
264 several days is typical of conditional null mutants for essential trypanosome genes (18). Evidence
265 for the expression of the MYC$_3$ tagged TbFUT1 protein in the BSF *TbFUT1*-MYC$_3$ cKO cell line

266 and of unmodified TbFUT1 in the BSF *TbFUT1* cKO cell line under permissive conditions is
267 shown in (Fig. 5*F*).

268 From a morphological point of view, both procyclic form *TbGMD* and *TbFUT1*
269 conditional null mutants grown under non-permissive conditions showed an increase in average
270 cell volume, due to increased cell length, concomitant with the start of the cell growth phenotype
271 (Fig. S9*A*). However, we were unable to reproduce the flagellar detachment phenotype previously
272 reported for the PCF *TbGMD* cKO grown in non-permissive conditions (26), nor was such a
273 phenotype observed in the PCF *TbFUT1* cKO parasites, either by scanning electron microscopy
274 or immunofluorescence (Fig. S9*C* and S10). The percentage of cells displaying flagellar
275 detachment (1.5-2 %) in both null mutants grown in non-permissive conditions (Fig. S9*B*) was
276 consistent with what has previously been reported for wild type cells (62). Additionally, we could
277 observe no defect in cell motility in either PCF *TbGMD* or PCF *TbFUT1* cKO grown in non-
278 permissive conditions (Fig. S11).

279

280 ***TbFUT1 localizes to the parasite mitochondrion.*** The BSF *TbFUT1*-MYC_3 cKO cell line, grown
281 under permissive conditions, was stained with anti-MYC antibodies and produced a pattern
282 suggestive of mitochondrial localization. This was confirmed by co-localization with
283 MitoTracker™ (Fig. 6*A*). However, when TbFUT1 was introduced into wild type cells fused with
284 an HA_3 epitope tag at the N-terminus, either with or without a C-terminal MYC_3-tag (constructs
285 pLEW100:HA_3-FUT1-MYC_3 and pLEW100:HA_3-FUT1), the tagged protein co-localized with
286 GRASP, a marker of the Golgi apparatus (Fig. 6*B* and *C*). In these cases, we suspect that N-
287 terminal tagging has disrupted mitochondrial targeting, by obscuring the N-terminal
288 mitochondrial targeting sequence. Indeed, no mitochondrial targeting motif was predicted *in*
289 *silico* for N-terminal HA_3 tagged TbFUT1. Nevertheless, since the mitochondrial localization of a

290 fucosyltransferase is unprecedented, we elected to raise polyclonal antibodies against
291 recombinant TbFUT1 to further assess its subcellular location. To do so, an N-terminally His_6-
292 tagged Δ_{32}TbFUT1 protein was expressed, re-solubilized from inclusion bodies and used for
293 rabbit immunization. The IgG fraction was isolated on immobilized protein-A and the anti-
294 TbFUT1 IgG sub-fraction affinity purified on immobilized recombinant GST-TbFUT1 fusion
295 protein. To further ensure mono-specificity of the antibodies to TbFUT1, the resulting fraction
296 was adsorbed against a concentrated cell lysate of the PCF *TbFUT1* cKO mutant grown for 9 days
297 under non-permissive conditions. The resulting highly-specific polyclonal antibody was used to
298 detect TbFUT1 expression in wild type bloodstream form cells as well as in BSF and PCF
299 *TbFUT1* cKO cells under permissive and non-permissive conditions (Fig. 7*A*-*C*). Anti-TbFUT1
300 antibodies co-localized with MitoTracker™ staining in the wild-type cells and in the conditional
301 null mutants under permissive conditions. No signal for the anti-TbFUT1 antibodies was seen
302 under non-permissive conditions, confirming the specificity of the polyclonal antibody. Taking
303 the possibility of a dual Golgi/mitochondrial localization into account, TbFUT1 localization was
304 also assessed in bloodstream form cells ectopically expressing TbGnTI-HA_3 as an authentic Golgi
305 marker (63). No co-localization between TbGnTI-HA_3 and anti-TbFUT1 was observed,
306 suggesting that TbFUT1 is either exclusively or predominantly expressed in the parasite
307 mitochondrion (Fig. 7*D*).
308
309 ***Deletion of TbFUT1 disturbs mitochondrial activity.*** Bloodstream form wild type and BSF
310 *TbFUT1* cKO cells, grown with and without tetracycline for 5 days, were stained with antibodies
311 to mitochondrial ATPase and with MitoTracker™. As expected ATPase and MitoTracker™ co-
312 localized in wild type cells and in the mutant under permissive conditions (Fig. 8, top panels).
313 However, under non-permissive conditions the few remaining viable cells showed significantly

314 diminished MitoTracker™ staining, indicative of reduced mitochondrial membrane potential, and
315 a reduction in ATPase staining, suggesting that TbFUT1 is in some way required for
316 mitochondrial function (Fig. 8, lower panels, and Fig. S12).
317

318 **DISCUSSION**

319 The presence and essentiality of the nucleotide sugar donor GDP-Fuc in BSF and PCF
320 trypanosomes lead us to search for putative FUTs in the parasite genome. Only one gene
321 (*TbFUT1*; Tb927.9.3600), belonging to the CAZy GT11 family, was found and phylogenetic
322 analyses revealed that one, or two in the case of *T. cruzi*, orthologues could be found in the
323 genomes of other kinetoplastids. These putative kinetoplastid FUTs form a distinct clade within
324 the GT11 FUT superfamily and are distinct from the GT10 FUTs found in *T. cruzi, L. major* and
325 related parasites, which are absent in *T. brucei*. Consistent with TbFUT1 being the only enzyme
326 likely to utilise the essential metabolite GDP-Fuc, we found that TbFUT1 is also essential to both
327 BSF and PCF parasites. We were able to express TbFUT1 in *E. coli* and the recombinant enzyme
328 was used to demonstrate its activity as a GDP-Fuc : βGal α-1,2 fucosyltransferase with a
329 preference for a Galβ1,3GlcNAcβ1-O-R acceptor motif out of the acceptor substrates
330 investigated.

331 The highly unusual result was the localization of TbFUT1 to the parasite mitochondrion,
332 using an affinity-purified antibody raised against native TbFUT1 as well as C-terminal epitope
333 tagging. Although in recent years fucosylation has been described in the nucleus and cytosol of
334 protists and plants (35, 36, 38, 64), we are unaware of any other examples of mitochondrial FUTs
335 in any organism. Mitochondrial glycosylation in general is poorly understood. The only other
336 known example of a mitochondrial-localized glycosyltransferase is mOGT (45). Mitochondria of
337 rat cardiomyocytes are also positive for OGA and express a UDP-GlcNAc transporter on their

338 outer membrane, indicating all of the molecular components required for this cycling post-
339 translational modification are present in the organelle (46). Interestingly, disruption of mOGT in
340 HeLa cell mitochondria also leads to mitochondrial disfunction. While there are no (m)OGT
341 orthologues in kinetoplastids, these observations highlight some of the challenges inherent for a
342 mitochondrial-localized glycosyltransferase. Firstly, for TbFUT1 to be active, GDP-Fuc needs to
343 be imported into the mitochondrion, suggesting the presence of an uncharacterized mitochondrial
344 GDP-sugar transporter. Secondly, TbFUT1 appears to be an α-1,2-FUT that decorates glycans
345 terminating in Galβ1,3GlcNAc, suggesting either that additional uncharacterized
346 glycosyltransferases and nucleotide sugar transporters may be present in the parasite
347 mitochondrion, or that the glycoconjugate substrate is assembled in the secretory pathway and
348 then somehow imported into the mitochondrion to be modified by TbFUT1. Experiments to
349 resolve these options will be undertaken, as will further experiments to try to find the protein,
350 lipid and/or other acceptor substrates of TbFUT1. The latter may then provide clues as to why
351 TbFUT1 is essential for mitochondrial function and parasite growth. Several attempts to identify
352 TbFUT1 substrates have failed so far, these include fucose-specific lectin blotting and pull-
353 downs, [^{3}H]fucose labelling of parasites transfected with GDP-Fuc salvage pathway enzymes and
354 LC-MS/MS precursor ion and neutral-loss scanning methods. Although the significance is
355 unclear, it is interesting to note that procyclic TbFUT1 has been recently shown to be under
356 circadian regulation (65).

357 In conclusion, *Tb*FUT1 is an essential, mitochondrial α-1,2-FUT with orthologues
358 throughout the kinetoplastidia. Although no data is available so far on the enzymes from other
359 members of this group, these initial results suggest the intriguing possibility of an essential,
360 conserved mitochondrial fucosylation pathway in kinetoplastids that might be exploitable as a
361 common drug target.

362

363 **EXPERIMENTAL PROCEDURES**

364 **Parasite strains.** *T. brucei* procyclic form (strain 427, clone 29.13) and bloodstream form (strain
365 427, variant MITaT 1.2) were used in these experiments. Both strains are stably expressing T7
366 polymerase and tetracycline repressor protein under G418 (bloodstream) or G418 and
367 hygromycin (procyclic) selection (66). Details on media and selection antibiotics can be found in
368 the SI Methods.

369

370 **Cloning, protein expression and purification of TbFUT1.** The putative *TbFUT1*
371 (Tb927.9.3600) was identified via BLASTp searches as described in Methods SI. The open
372 reading frame (ORF) was amplified by PCR from *T. brucei* strain 427 genomic DNA and cloned
373 into the N-terminal GST fusion vector pGEX-6P-1, modified to contain the PreScission Protease
374 site (kind gift of Prof. Daan Van Aalten). The resulting pGEX6P1-GST-PP-*Tb*FUT1 was
375 transformed into BL21 (DE3) *E. coli* strain. Recombinant protein expression was induced with
376 isopropyl-β-D-thiogalactopyranoside (IPTG) and carried out at 16°C for 16 h. GST-TbFUT1 was
377 isolated from the soluble fraction by affinity purification with Glutathione Sepharose Fast Flow
378 beads. Recombinant protein identification by peptide mass fingerprinting was performed by the
379 Proteomic and Mass Spectrometry facility, School of Life Sciences, University of Dundee.
380 Primer sequences and details on cloning, expression, and purification can be found in the SI
381 Methods.

382

383 **Fucosyltransferase activity assays.** Aliquots of 2 µg of affinity purified GST-TbFUT1 were
384 incubated with 1 µCi GDP[^{3}H]Fuc (American Radiochemicals), 1 mM acceptor in 50 mM Tris-
385 HCl, 25 mM KCl, 5 mM $MgCl_2$, 5 mM $MnCl_2$, pH 7.2 for 2 h at 37°C. The acceptors tested

386 (Table 1) were purchased from Sigma, Dextra Laboratories or Toronto Research Chemicals. To
387 study the dependency on divalent cations, $MgCl_2$ and $MnCl_2$ were removed from the buffer and a
388 formulation with 10 mM EDTA was also tested. Reactions were stopped by cooling on ice, then
389 desalted on mixed bed columns as detailed in SI Methods. About 5% of the desalted reactions
390 were counted at a LS 6500 scintillation counter (Beckmann). The remaining material was
391 lyophilized for further analyses.
392
393 **HPTLC analysis**. Reaction products and standards were dissolved in 20% 1-propanol and
394 separated on a 10 cm HPTLC Si-60 plates (Merck) using 1-propanol:acetone:water 9:6:4 (v:v:v)
395 as mobile phase. Non-radiolabelled sugars were visualized by orcinol/ H_2SO_4 staining. In the case
396 of radiolabelled products, the HPTLC plates were sprayed with En^{3}hance® (PerkinElmer) and
397 visualized by fluorography.
398
399 **Large scale TbFUT1 assay and product purification.** Acceptor (5 mM Lacto-N-biose-β-O-
400 methyl) and donor (2.5 mM GDP-Fuc) were incubated with 8 µg affinity purified GST-TbFUT1
401 in 20 mM Tris-HCl, 25 mM KCl, pH 7.2 at 37°C for 24 h. The reaction products were desalted on
402 a mixed-bed column and lyophilized. The trisaccharide product was isolated by normal phase
403 liquid chromatography on an amino column as described in Methods SI. The fractions containing
404 the putative trisaccharide product were pooled and lyophilized.
405
406 **Permethylation, ESI-MS analysis and GC-MC methylation linkage analysis.** Purified
407 TbFUT1 reaction product was dried and permethylated by the sodium hydroxide method as
408 described in (68). Aliquots were used for ESI-MS and the remainder was subjected to acid
409 hydrolysis followed by NaB^2H_4 reduction and acetylation (67). The resulting PMAAs were

410 analysed using an HP6890 GC System equipped with an HP-5 column linked to a 5975C mass
411 spectrometer (Agilent). For ESI-MS and ESI-MS/MS, the permethylated glycans were directly
412 infused into a Q-Star XL mass spectrometer equipped with Analyst software (Applied
413 Biosystems). See Methods SI for details.
414
415 **NMR.** The purified TbFUT1 reaction product was exchanged in $^{2}H_2O$ by freeze-drying and
416 analysed by one-dimensional ^{1}H-NMR and two-dimensional ^{1}H-ROESY (Rotating frame
417 Overhouser Effect SpectroscopY). All spectra were acquired on a Bruker Avance spectrometer
418 operating at 500 MHz with a probe temperature of 293°K.
419
420 **Generation of *TbFUT1* conditional null mutants.** About 500 bp of the 5' and 3' untranslated
421 regions (UTRs) immediately flanking the *TbFUT1* ORF were amplified from *T. brucei* genomic
422 DNA (gDNA) and linked together by PCR. Antibiotic resistance cassettes were cloned into the
423 *Hind*III/*BamH*I restriction sites between the two UTRs to generate constructs either containing
424 puromycin acetyltransferase (*PAC*) or blastacidin S deamidase (*BSD*). In addition, a hygromycin
425 (HYG) based *TbFUT1* gene replacement cassette was generated with longer UTRs (1.25 kb). The
426 tetracycline-inducible ectopic copy construct was generated by amplifying the *TbFUT1* ORF
427 from *T. brucei* gDNA and cloning the resulting PCR product into pLEW100. Additionally, a
428 modified pLEW100 vector was generated which allowed universal tagging of a protein of interest
429 with a C-terminal 3x MYC tag. Linearized DNA was used to transform the parasites as
430 previously described (66, 68, 69). The genotype of the transformed parasites was verified by
431 Southern blot. For details see Methods SI.
432

433 **Northern blotting**. Total RNA was prepared from $5x10^6$-$1x10^7$ cells using the RNeasy MIDI Kit
434 (Qiagen) according to manufacturer's instructions. The RNA was separated on a 2% agarose-
435 formaldehyde gel, blotted and detected using the Northern Starter Kit (Roche). Probes were
436 designed based on the DIG RNA Labelling Kit T7 (Roche) and *TbFUT1* and alpha-tubulin
437 (Tb427.01.2340) templates were amplified from *T. brucei* bloodstream form gDNA using primers
438 P17/P18 and P19/P20 (Table S2), respectively. Total RNA and DIG labelled probes were quality
439 checked by capillary electrophoresis on an Agilent BioAnalyzer 2100.
440
441 **Generation and expression of epitope-tagged TbFUT1 constructs.** *TbFUT1* was introduced in
442 two different sites of pLEW100HXM (see Methods SI) to yield HA_3-TbFUT1 and HA_3-TbFUT1-
443 MYC_3. TbFUT1 was amplified using primers P21/P22 for HA_3-TbFUT1 and P23/P16 for HA_3-
444 TbFUT1-MYC_3 (Table S2). The two plasmids were purified and electroporated into BSF cells as
445 described above. The generation of the TbFUT1-MYC_3 cell line is described above as it was used
446 to generate the BSF *TbFUT1* cKO cell line.
447
448 **Preparation of anti-FUT1 antibody**. An N-terminally truncated construct encoding Δ_{32}TbFUT1
449 fused to an N-terminal hexahistidine tag (HIS_6) with PreScission plus (PP) protease cleavage site
450 in a pET15b expression vector was introduced into BL21 (DE3) gold *E.coli* cells. *E. coli* cells
451 were allowed to express His_6-PP-TbFUT1 over night at 25°C in auto-inducing media (5052-NPS-
452 $MgSO_4$). The recombinant HIS_6-PP-Δ_{32}TbFUT1 protein was resolubilized from inclusion bodies
453 as described in Methods SI. Re-solubilised protein (2 mg) was sent off to DC Biosciences ^{LTD} for
454 production of polyclonal rabbit antiserum. See Methods SI for details on the purification of the
455 anti-TbFUT1 IgG fraction.
456

457 **Immunofluorescence microscopy.** Late log phase *T. brucei* bloodstream form or procyclic cells
458 were fixed in 4% PFA/PBS in solution. When using Mitotracker™ Red CMX Ros cell cultures
459 were spiked with a 25 nM concentration over 20 minutes, before harvesting. Permeabilization,
460 blocking and labelling conditions are described in Methods SI. Microscopy was performed on a
461 DeltaVision Spectris microscope (GE Healthcare) and images were processed using Softworx.
462

463 **ACKNOWLEDGEMENTS**

464 The authors would like to thank Gina MacKay and Art Crossman (University of Dundee) for
465 performing the NMR experiment and helping with the data analysis. We would also like to thanks
466 Alan R. Prescott (Division of Cell Signalling and Immunology, University of Dundee) for his
467 generous help with the confocal microscopy and Martin Kierans for preparing the samples for
468 scanning electron microscopy. The authors are also grateful to Keith Gull (University of Oxford),
469 Graham Warren (University College London), Daan van Aalten and David Horn (University of
470 Dundee) for providing reagents. This work was supported by a University of Dundee/BBSRC
471 PhD studentship to G.B. and by a Wellcome Trust Investigator Award (101842) to M.A.J.F.
472

473 **REFERENCES**

474 1. Matthews KR (2005) The developmental cell biology of *Trypanosoma brucei. J Cell Sci*
475 118(Pt 2):283–290.

476 2. Cross GAM (1996) Antigenic variation in trypanosomes: Secrets surface slowly. *Bioessays*
477 18(4):283–291.

478 3. Pays E (1998) Expression and function of surface proteins in *Trypanosoma brucei*. *Mol*
479 *Biochem Parasitol* 91(1):3–36.

480 4. Mehlert A, Richardson JM, Ferguson MA (1998) Structure of the
481 glycosylphosphatidylinositol membrane anchor glycan of a class-2 variant surface
482 glycoprotein from *Trypanosoma brucei*. *J Mol Biol* 277(2):379–392.

483 5. Schwede A, Carrington M (2010) Bloodstream form trypanosome plasma membrane
484 proteins: antigenic variation and invariant antigens. *Parasitology* 137(14):2029–2039.

485 6. Richardson JP, Beecroft RP, Tolson DL, Liu MK, Pearson TW (1988) Procyclin: an unusual
486 immunodominant glycoprotein surface antigen from the procyclic stage of African
487 trypanosomes. *Mol Biochem Parasitol* 31(3):203–216.

488 7. Treumann A, et al. (1997) Structural characterisation of two forms of procyclic acidic
489 repetitive protein expressed by procyclic forms of *Trypanosoma brucei. J Mol Biol*
490 269(4):529–547.

491 8. Roditi I, Furger A, Ruepp S, Schürch N, Bütikofer P (1998) Unravelling the procyclin coat
492 of *Trypanosoma brucei. Mol Biochem Parasitol* 91(1):117–130.

493 9. Vassella E, et al. (2001) Multiple procyclin isoforms are expressed differentially during the
494 development of insect forms of *Trypanosoma brucei. J Mol Biol* 312(4):597–607.

495 10. Vassella E, Bütikofer P, Engstler M, Jelk J, Roditi I (2003) Procyclin null mutants of
496 *Trypanosoma brucei* express free glycosylphosphatidylinositols on their surface. *Mol Biol*
497 *Cell* 14(4):1308–1318.

498 11. Roper JR (2005) The Suppression of Galactose Metabolism in Procyclic Form *Trypanosoma*

499 *brucei* Causes Cessation of Cell Growth and Alters Procyclin Glycoprotein Structure and
500 Copy Number. *J Biol Chem* 280(20):19728–19736.

501 12. Nagamune K, et al. (2004) Surface Sialic Acids Taken from the Host Allow Trypanosome
502 Survival in Tsetse Fly Vectors. *J Exp Med* 199(10):1445–1450.

503 13. Güther MLS, et al. (2009) Fate of glycosylphosphatidylinositol (GPI)-less procyclin and
504 characterization of sialylated non-GPI-anchored surface coat molecules of procyclic-form
505 *Trypanosoma brucei*. *Eukaryot Cell* 8(9):1407–1417.

506 14. Nagamune K, et al. (2000) Critical roles of glycosylphosphatidylinositol for *Trypanosoma*
507 *brucei*. *Proc Natl Acad Sci USA* 97(19):10336–10341.

508 15. Chang T, Milne KG, Güther MLS, Smith TK, Ferguson MAJ (2002) Cloning of
509 *Trypanosoma brucei* and *Leishmania major* genes encoding the GlcNAc-
510 phosphatidylinositol de-N-acetylase of glycosylphosphatidylinositol biosynthesis that is
511 essential to the African sleeping sickness parasite. *J Biol Chem* 277(51):50176–50182.

512 16. Smith TK, Crossman A, Brimacombe JS, Ferguson MAJ (2004) Chemical validation of GPI
513 biosynthesis as a drug target against African sleeping sickness. *EMBO J* 23(23):4701–4708.

514 17. Urbaniak MD, Crossman A, Ferguson MAJ (2008) Probing *Trypanosoma brucei*
515 Glycosylphosphatidylinositol Biosynthesis Using Novel Precursor-Analogues. *Chem Biol*
516 *Drug Des* 72(2):127–132.

517 18. Roper JR, Guther MLS, Milne KG, Ferguson MAJ (2002) Galactose metabolism is essential
518 for the African sleeping sickness parasite *Trypanosoma brucei*. *Proc Natl Acad Sci USA*
519 99(9):5884–5889.

520 19. Urbaniak MD, Turnock DC, Ferguson MAJ (2006) Galactose starvation in a bloodstream
521 form *Trypanosoma brucei* UDP-glucose 4'-epimerase conditional null mutant. *Eukaryot*
522 *Cell* 5(11):1906–1913.

523 20. Urbaniak MD, et al. (2006) Identification of novel inhibitors of UDP-Glc 4′-epimerase, a
524 validated drug target for african sleeping sickness. *Bioorg Med Chem Lett* 16(22):5744–
525 5747.

526 21. Stokes MJ, et al. (2008) The Synthesis of UDP-N-acetylglucosamine Is Essential for
527 Bloodstream Form *Trypanosoma brucei* in Vitro and in Vivo and UDP-N-acetylglucosamine
528 Starvation Reveals a Hierarchy in Parasite Protein Glycosylation. *J Biol Chem*
529 283(23):16147–16161.

530 22. Denton H, Fyffe S, Smith TK (2010) GDP-mannose pyrophosphorylase is essential in the
531 bloodstream form of *Trypanosoma brucei*. *Biochem J* 425(3):603–614.

532 23. Marino K, et al. (2011) Characterization, Localization, Essentiality, and High-Resolution
533 Crystal Structure of Glucosamine 6-Phosphate N-Acetyltransferase from *Trypanosoma*
534 *brucei*. *Eukaryot Cell* 10(7):985–997.

535 24. Marino K, et al. (2010) Identification, subcellular localization, biochemical properties, and
536 high-resolution crystal structure of *Trypanosoma brucei* UDP-glucose pyrophosphorylase.
537 *Glycobiology* 20(12):1619–1630.

538 25. Turnock DC, Ferguson MAJ (2007) Sugar nucleotide pools of *Trypanosoma brucei,*
539 *Trypanosoma cruzi*, and *Leishmania major*. *Eukaryot Cell* 6(8):1450–1463.

540 26. Turnock DC, Izquierdo L, Ferguson MAJ (2007) The de novo synthesis of GDP-fucose is
541 essential for flagellar adhesion and cell growth in *Trypanosoma brucei*. *J Biol Chem*
542 282(39):28853–28863.

543 27. Guo H, et al. (2017) Genetic metabolic complementation establishes a requirement for GDP-
544 fucose in *Leishmania*. *J Biol Chem* 292(25):10696–10708.

545 28. Cooper R, de Jesus AR, Cross GA (1993) Deletion of an immunodominant *Trypanosoma*
546 *cruzi* surface glycoprotein disrupts flagellum-cell adhesion. *J Cell Biol* 122(1):149–156.

547 29. Haynes PA, Ferguson MA, Cross GA (1996) Structural characterization of novel
548 oligosaccharides of cell-surface glycoproteins of *Trypanosoma cruzi*. *Glycobiology*
549 6(8):869–878.

550 30. Allen S, Richardson JM, Mehlert A, Ferguson MAJ (2013) Structure of a complex
551 phosphoglycan epitope from gp72 of *Trypanosoma cruzi*. *J Biol Chem* 288(16):11093–
552 11105.

553 31. Coutinho PM, Deleury E, Davies GJ, Henrissat B (2003) An Evolving Hierarchical Family
554 Classification for Glycosyltransferases. *J Mol Biol* 328(2):307–317.

555 32. Lombard V, Golaconda Ramulu H, Drula E, Coutinho PM, Henrissat B (2013) The
556 carbohydrate-active enzymes database (CAZy) in 2013. *Nucleic Acids Res* 42(D1):D490–
557 D495.

558 33. Martinez-Duncker I (2003) A new superfamily of protein-*O*-fucosyltransferases, 2-
559 fucosyltransferases, and 6-fucosyltransferases: phylogeny and identification of conserved
560 peptide motifs. *Glycobiology* 13(12):1C–5.

561 34. Breton C, Oriol R, Imberty A (1998) Conserved structural features in eukaryotic and
562 prokaryotic fucosyltransferases. *Glycobiology* 8(1):87–94.

563 35. Rahman K, et al. (2016) The E3 Ubiquitin Ligase Adaptor Protein Skp1 Is Glycosylated by
564 an Evolutionarily Conserved Pathway That Regulates Protist Growth and Development. *J*
565 *Biol Chem* 291(9):4268–4280.

566 36. Van Der Wel H, Fisher SZ, West CM (2002) A bifunctional diglycosyltransferase forms the
567 Fucalpha1,2Galbeta1,3-disaccharide on Skp1 in the cytoplasm of *Dictyostelium*. *J Biol*
568 *Chem* 277(48):46527–46534.

569 37. West CM, Wang ZA, Van Der Wel H (2010) A cytoplasmic prolyl hydroxylation and
570 glycosylation pathway modifies Skp1 and regulates O2-dependent development in
571 *Dictyostelium*. *Biochim Biophys Acta* 1800(2):160–171.

572 38. Zentella R, et al. (2017) The *Arabidopsis O*-fucosyltransferase SPINDLY activates nuclear
573 growth repressor DELLA. *Nat Chem Biol* 161:1279.

574 39. Gas-Pascual E, et al. (2019) CRISPR/Cas9 and glycomics tools for *Toxoplasma*
575 glycobiology. *J Biol Chem* 294(4):1104–1125.

576 40. Priest JW, Hajduk SL (1994) Developmental regulation of mitochondrial biogenesis in
577 *Trypanosoma brucei*. *J Bioenerg Biomembr* 26(2):179–191.

578 41. Jensen RE, Englund PT (2012) Network news: the replication of kinetoplast DNA. *Annu*

579 *Rev Microbiol* 66:473–491.

580 42. Povelones ML (2014) Beyond replication: Division and segregation of mitochondrial DNA
581 in kinetoplastids. *Mol Biochem Parasitol* 196(1):53–60.

582 43. Ogbadoyi EO, Robinson DR, Gull K (2003) A high-order trans-membrane structural linkage
583 is responsible for mitochondrial genome positioning and segregation by flagellar basal
584 bodies in trypanosomes. *Mol Biol Cell* 14(5):1769–1779.

585 44. Kung LA, et al. (2009) Global analysis of the glycoproteome in *Saccharomyces cerevisiae*
586 reveals new roles for protein glycosylation in eukaryotes. *Mol Syst Biol* 5:308.

587 45. Bond MR, Hanover JA (2015) A little sugar goes a long way: the cell biology of *O*-GlcNAc.
588 *J Cell Biol* 208(7):869–880.

589 46. Banerjee PS, Ma J, Hart GW (2015) Diabetes-associated dysregulation of *O*-GlcNAcylation
590 in rat cardiac mitochondria. *Proc Natl Acad Sci U S A* 112(19):6050–6055.

591 47. Sacoman JL, Dagda RY, Burnham-Marusich AR, Dagda RK, Berninsone PM (2017)
592 Mitochondrial *O*-GlcNAc Transferase (mOGT) Regulates Mitochondrial Structure,
593 Function, and Survival in HeLa Cells. *J Biol Chem* 292(11):4499–4518.

594 48. Zhang L, et al. (2010) *Helicobacter hepaticus* Hh0072 gene encodes a novel 1-3-
595 fucosyltransferase belonging to CAZy GT11 family. *Glycobiology* 20(9):1077–1088.

596 49. Wang G, Boulton PG, Chan NW, Palcic MM, Taylor DE (1999) Novel *Helicobacter pylori*
597 alpha1,2-fucosyltransferase, a key enzyme in the synthesis of Lewis antigens. *Microbiology*
598 145 (Pt 11)(11):3245–3253.

599 50. Kelly RJ, Rouquier S, Giorgi D, Lennon GG, Lowe JB (1995) Sequence and expression of a
600 candidate for the human Secretor blood group alpha(1,2)fucosyltransferase gene (FUT2).
601 Homozygosity for an enzyme-inactivating nonsense mutation commonly correlates with the
602 non-secretor phenotype. *J Biol Chem* 270(9):4640–4649.

603 51. Li M, et al. (2008) Characterization of a Novel α1,2-Fucosyltransferase of *Escherichia coli*
604 O128:B12 and Functional Investigation of Its Common Motif. *Biochemistry* 47(1):378–387.

605 52. Takahashi T, et al. (2000) A sequence motif involved in the donor substrate binding by
606 alpha1,6-fucosyltransferase: the role of the conserved arginine residues. *Glycobiology*
607 10(5):503–510.

608 53. Horton P, Nakai K (1997) Better prediction of protein cellular localization sites with the k
609 nearest neighbors classifier. *Proc Int Conf Intell Syst Mol Biol* 5:147–152.

610 54. Emanuelsson O, Nielsen H, Brunak S, von Heijne G (2000) Predicting Subcellular
611 Localization of Proteins Based on their N-terminal Amino Acid Sequence. *J Mol Biol*
612 300(4):1005–1016.

613 55. Claros MG, Vincens P (1996) Computational method to predict mitochondrially imported
614 proteins and their targeting sequences. *Eur J Biochem* 241(3):779–786.

615 56. Krnáčová K, Vesteg M, Hampl V, Vlček Č, Horváth A (2012) Euglena gracilis and
616 Trypanosomatids possess common patterns in predicted mitochondrial targeting
617 presequences. *J Mol Evol* 75(3-4):119–129.

618 57. Long S, Jirku M, Ayala FJ, Lukes J (2008) Mitochondrial localization of human frataxin is
619 necessary but processing is not for rescuing frataxin deficiency in *Trypanosoma brucei*.
620 *Proc Natl Acad Sci U S A* 105(36):13468–13473.

621 58. Aslett M, et al. (2009) TriTrypDB: a functional genomic resource for the Trypanosomatidae.
622 *Nucleic Acids Res* 38(suppl_1):D457–D462.

623 59. Beyer TA, Hill RL (1980) Enzymatic-Properties of the Beta-Galactoside-Alpha-1-] 2
624 Fucosyl-Transferase From Porcine Sub-Maxillary Gland. *J Biol Chem* 255(11):5373–5379.

625 60. Kamińska J, Wiśniewska A, Kościelak J (2003) Chemical modifications of α1,6-
626 fucosyltransferase define amino acid residues of catalytic importance. *Biochimie* 85(3-
627 4):303–310.

628 61. Pettit N, et al. (2010) Characterization of WbiQ: An α1,2-fucosyltransferase from
629 *Escherichia coli* O127:K63(B8), and synthesis of H-type 3 blood group antigen. *Biochem*
630 *Biophys Res Commun* 402(2):190–195.

631 62. LaCount DJ, Barrett B, Donelson JE (2002) *Trypanosoma brucei* FLA1 Is Required for
632 Flagellum Attachment and Cytokinesis. *J Biol Chem* 277(20):17580–17588.

633 63. Damerow M, et al. (2014) Identification and Functional Characterization of a Highly
634 Divergent *N*-Acetylglucosaminyltransferase I (TbGnTI) in *Trypanosoma brucei*. *J Biol*
635 *Chem* 289(13):9328–9339.

636 64. Bandini G, et al. (2016) *O*-fucosylated glycoproteins form assemblies in close proximity to
637 the nuclear pore complexes of *Toxoplasma gondii*. *Proc Natl Acad Sci USA* 113(41):11567–
638 11572.

639 65. Rijo-Ferreira F, Pinto-Neves D, Barbosa-Morais NL, Takahashi JS, Figueiredo LM (2017)
640 *Trypanosoma brucei* metabolism is under circadian control. *Nature Microbiol* 2:17032.

641 66. Wirtz E, Leal S, Ochatt C, Cross GA (1999) A tightly regulated inducible expression system
642 for conditional gene knock-outs and dominant-negative genetics in *Trypanosoma brucei*.
643 *Mol Biochem Parasitol* 99(1):89–101.

644 67. Ferguson MAJ (1992) Chemical and enzymatic analysis of glycosylphosphoditylinositol
645 anchors. *Lipid Modification of Proteins: A Practical Approach* (IRL Press, Oxford), pp 191–
646 230.

647 68. Burkard G, Fragoso CM, Roditi I (2007) Highly efficient stable transformation of
648 bloodstream forms of *Trypanosoma brucei. Mol Biochem Parasitol* 153(2):220–223.

649 69. Güther MLS, Lee S, Tetley L, Acosta-Serrano A, Ferguson MAJ (2006) GPI-anchored
650 proteins and free GPI glycolipids of procyclic form *Trypanosoma brucei* are nonessential for
651 growth, are required for colonization of the tsetse fly, and are not the only components of the
652 surface coat. *Mol Biol Cell* 17(12):5265–5274.

653

654

655 Table 1. Acceptor substrates and semi-quantitative fucosyltransferase activities.

*Tb*FUT1 Activity	Lane of Fig. 1	Abbreviat.	Name	Structure
+++	2, 5, 8	LNB	lacto-N-biose	**Galβ1,3GlcNAc**
+++	23	LNB-OMe	lacto-N-biose-O-methyl	**Galβ1,3GlcNAc**β-OMe
++	13	LNT	lacto-N-tetraose	**Galβ1,3GlcNAc**β1,3Galβ1,4Glc
++	16	LNH	lacto-N-hexaose	**Galβ1,3GlcNAc**β1,3(Galβ1,4GlacNAcβ1,6)Galβ1,4Glc
++	1	Lac	lactose	Galβ1,4Glc
+	15	iLNO	iso-lacto-N-octaose	**Galβ1,3GlcNAc**β1,3(**Galβ1,3GlacNAc**β1,3Galβ1,4GlcNAcβ1,6)Galβ1,4Glc
+	3	LacNAc	N-acetyllactosamine	Galβ1,4GlcNAcN
+	12	LNnH	lacto-N-neohexaose	Galβ1,4GlcNAcβ1,3(Galβ1,4GlcNAcβ1,6)Galβ1,4Glc
+	14	LNnT	lacto-N-neotetraose	Galβ1,4GlcNAcβ1,3Galβ1,4Glc
+	18	3'-FL	3'-fucosyllactose	Galβ1,4(Fucα1,3)Glc
-	11	β-Gal	β-galactose	β-Gal
-	17	GNG	β1,6-galactosyl-N-acetyl -glucosamine	Galβ1,6GlcNAc
-	19	1,6GB	β1,6-galactobiose	Galβ1,6Gal
-	20	1,4GB	galabiose	Galα1,4Gal
-	21	LB2TS	Linear B2 trisaccharide	Galα1,3Galβ1,4GlcNAc
-	22	β-Gal-OMe	β-galactose-O-methyl	β-Gal-OMe
-	24	2'-FL	2'-fucosyllactose	Fucα1,2Galβ1,4Glc

656 [a] The relative efficiencies of the acceptors to act as substrates (+++, ++, + and -) are based on visual
657 inspection of the intensities of the products bands in Figure 1.
658

659 Table 2. PMAAs derivatives identified by GC-MS methylation linkage analysis of the purified

660 TbFUT1 reaction product.

PMAA derivative	RT (min)	Origin
4,6-di-*O*-methyl-1,3,5-Tri-*O*-acetyl-(1-^{2}H)- 2-N-methylacetamidoglucosaminitol	24.6	3-*O*-substituted GlcNAc
2,3,4,6-tetra-*O*-methyl-1,5-di-*O*-acetyl-(1-^{2}H)-galactitol	16.7	Non-reducing terminal Gal
3,4,6-tri-*O*-methyl-1,2,5-tri-*O*-acetyl-(1-^{2}H)-galactitol	18.6	2-*O*-substituted Gal
2,3,4-tri-*O*-methyl-1,5-di-*O*-acetyl-(1-^{2}H)-fucositol	14.1	Non-reducing terminal Fuc
3,4-di-*O*-methyl-1,2,5-tri-*O*-acetyl-(1-^{2}H)-fucositol	15.9	2-*O*-substituted Fuc

661 RT: retention time

662

663 Table 3. ^{1}H and ^{1}H ROESY chemical shift assignments for the purified TbFUT1 reaction product.
664

Residue	H_1	H_2	H_3	H_4	H_5	$H_{6/6'}$	NAc
αFuc	5.05 (J=4 Hz)	3.57	3.67	3.63	4.2	1.1	
βGal	4.5	3.45	3.55	3.89	ND	ND	
βGlcNAc	ND	3.63	ND	3.4	ND	3.78/3.89	2.1

665
666
667 J: coupling
668 ND: chemical shift could not be clearly assigned
669
670

671 **FIGURE LEGENDS**

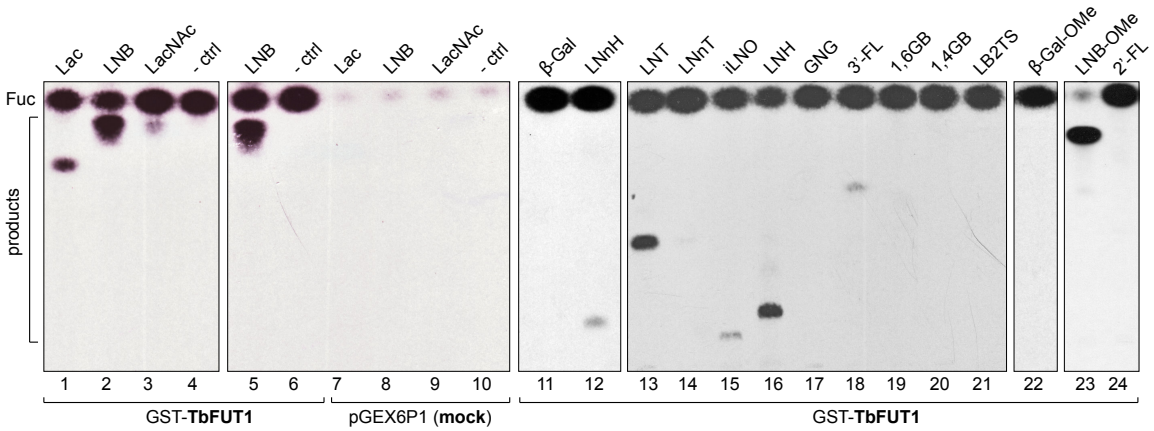

672

673 FIGURE 1. **Recombinant GST-TbFUT1 transfers [^{3}H]Fuc to a variety of sugar acceptors.**

674 Each assay used 2 µg of purified GST-TbFUT1, GDP-[^{3}H]Fuc and 1 mM of acceptor. Reaction

675 products were desalted and separated by silica HPTLC, and detected by fluorography. The

676 acceptor abbreviations above each lane are defined in Table 1. - *ctrl*: negative control reaction

677 missing the acceptor.

678

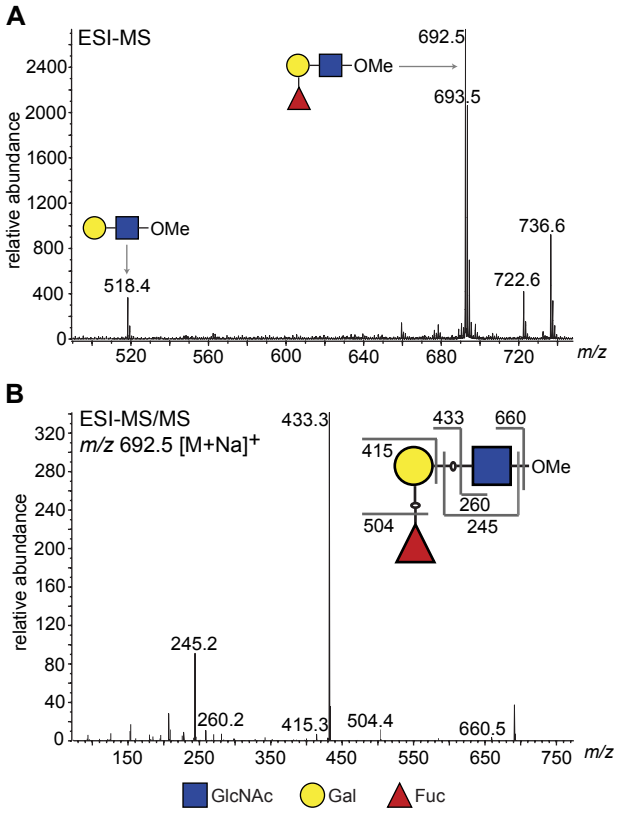

679

680 FIGURE 2. **ESI-MS and ESI-MS/MS of TbFUT1 *in vitro* reaction product**. *A*. ESI-MS of the
681 purified and permethylated reaction product. The ion at *m/z* 692.5 is consistent with the [M +
682 $Na]^+$ ion of a permethylated trisaccharide of composition $dHex_1Hex_1HexNAc_1$. Some of the
683 unmodified acceptor ($Hex_1HexNAc_1$) could still be observed (*m/z* 518.4). *B*. MS/MS product ion
684 spectrum of *m/z* 692.5. The collision-induced fragmentation pattern indicated that the dHex (Fuc)
685 residue was linked to the Hex (Gal) and not to the HexNAc (GlcNAc) residue.

686

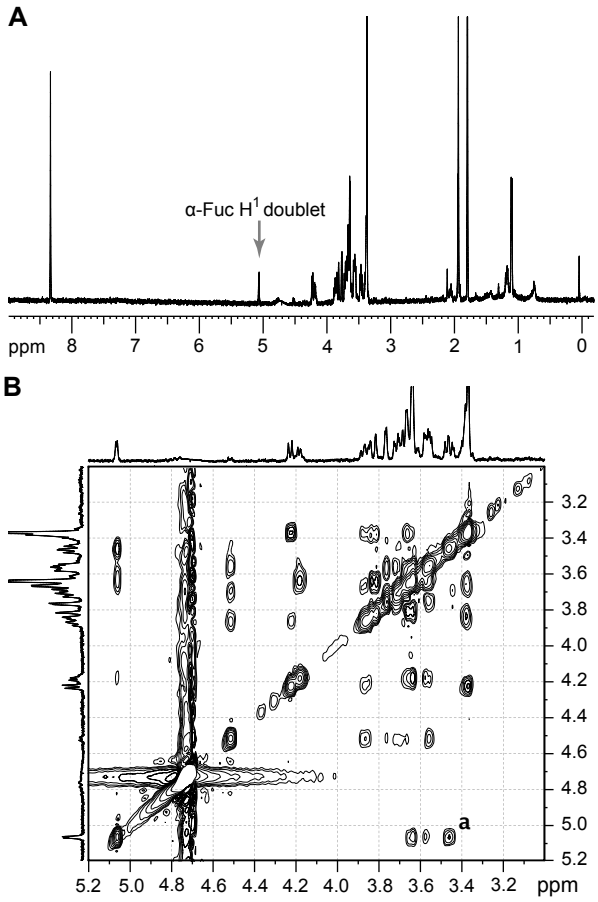

FIGURE 3. **^{1}H NMR and ^{1}H ROESY spectra of the TbFUT1 reaction product.** *A*. One-dimensional ^{1}H-NMR spectrum. The *arrow* points to the α-Fuc H_1 doublet. *B*. Enlargement of the 3.2-5.1 ppm region of the two-dimensional ^{1}H ROESY. ***a*** indicates the signal for a crosspeak resulting from a through-space connectivity between α-Fuc H_1 and β-Gal H_2.

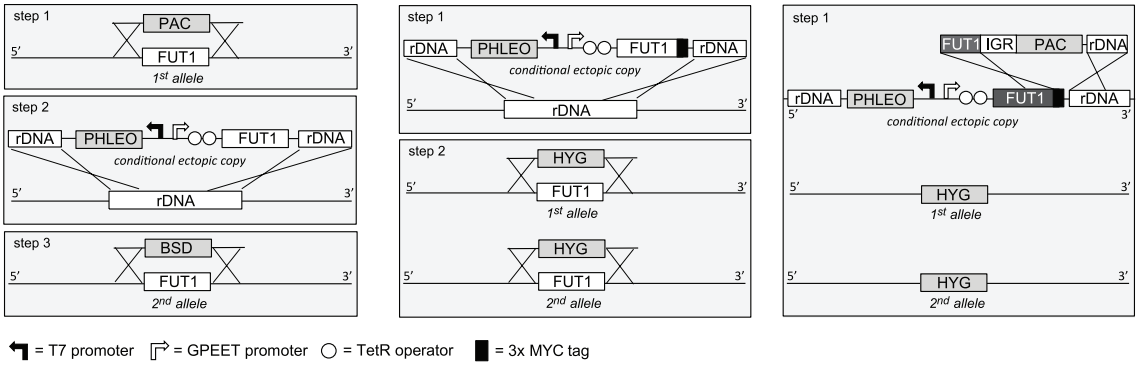

FIGURE 4. **Cloning strategies for the creation of the *TbFUT1* conditional null mutants**. *Left panel*: To create the procyclic form conditional null mutant (PCF *TbFUT1* cKO) the first *TbFUT1* allele was replaced by *PAC*, an ectopic tetracycline-inducible copy of the *TbFUT1* gene was introduced into the ribosomal DNA locus and the second *TbFUT1* allele was replaced by *BSD*. *Middle panel*: To create the bloodstream form conditional null mutant (BSF *TbFUT1-MYC$_3$* cKO) an ectopic tetracycline-inducible copy of the *TbFUT1* gene with a MYC$_3$ tag was first introduced into the ribosomal DNA locus. Both *TbFUT1* alleles were subsequently replaced by *HYG* through homologous recombination followed by gene conversion. *Right panel:* To create the untagged bloodstream form cKO (BSF *TbFUT1* cKO), the BSF *TbFUT1-MYC$_3$* cKO mutant (*middle panel*) was modified by homologous recombination with a construct that removed the C-terminal MYC$_3$ tag under *PAC* selection.

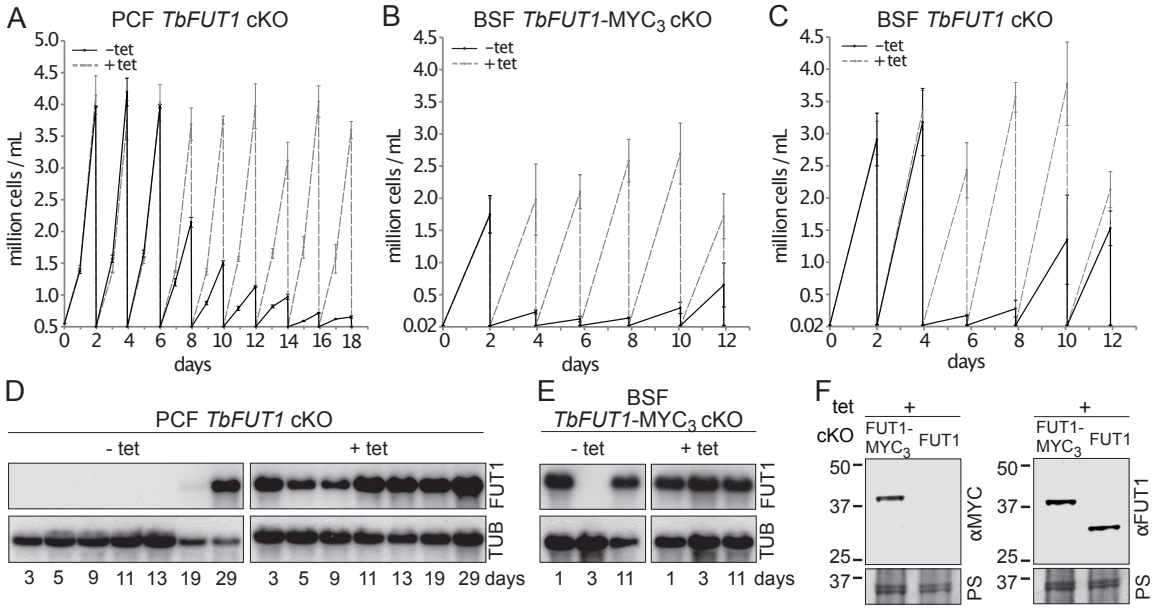

FIGURE 5. **TbFUT1 is essential for procyclic and bloodstream form cell growth *in vitro.*** The cell numbers (± standard deviation) for TbFUT1 cKO under permissive (plus tetracycline, *dotted line*) and non-permissive (minus tetracycline, *solid line*) conditions are shown for three procyclic (*A*) and bloodstream form (*C*) clones, as well as for three bloodstream clones carrying a tetracycline-inducible ectopic *TbFUT1* gene with a C-terminal MYC_3 tag (*B*). *D-E*. Corresponding *TbFUT1* mRNA levels were determined by Northern blots. Alpha-Tubulin (TUB) was used as a loading control. *F*. TbFUT1-MYC_3 and untagged TbFUT1 are detected by Western blot analysis in the respective bloodstream form cKO cell lines under permissing conditions (+ Tet). The *left panel* shows an anti-MYC (αMYC) blot and the *right panel* an anti-recombinant TbFUT1 antibody (αFUT1) blot. Membranes were stained with Ponceau S (PS) to ensure equal loading.

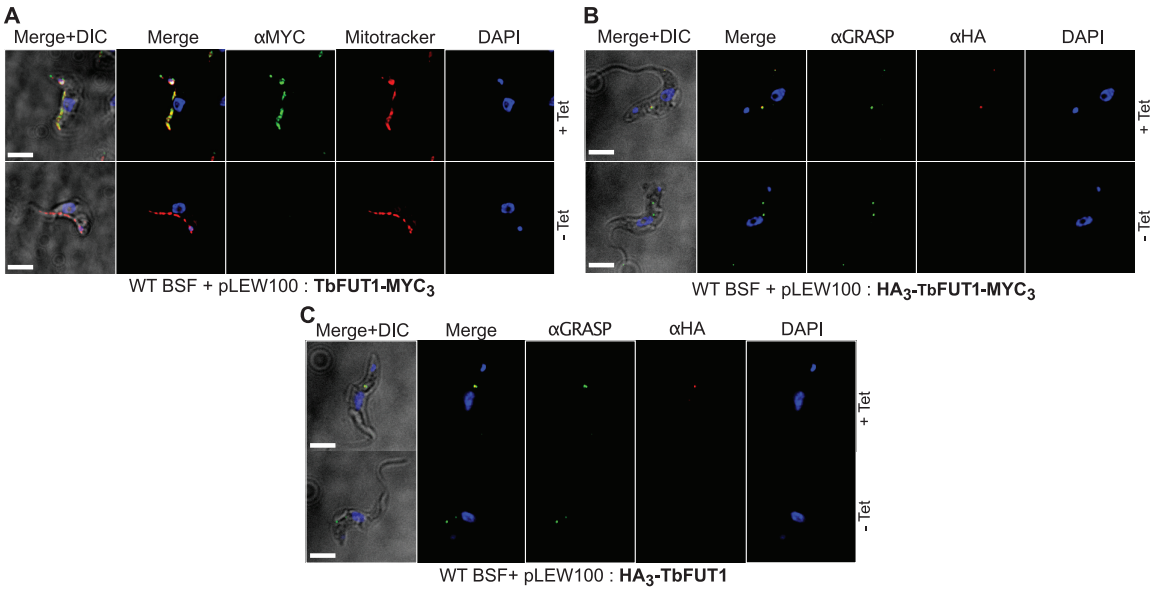

FIGURE 6. **The C- and N-terminal tagging of TbFUT1 result in mitochondrial and Golgi apparatus localization, respectively**. *A.* Bloodstream form (BSF) cKO parasites expressing tet-inducible C-terminally tagged TbFUT1-MYC_3 were imaged under permissive (+Tet) and non-permissive (-Tet) conditions by DIC and fluorescence microscopy after staining with anti-MYC, MitoTracker™, and DAPI. Comparable patterns were observed for anti-MYC and MitoTracker™, suggesting TbFUT1-MYC_3 localizes to the mitochondrion. *B-C*. IFA of BSF cKO parasites expressing a tet-inducible N-terminally tagged HA_3-TbFUT1-MYC_3 (*B*) or HA_3-TbFUT1 (*C*) after labelling with anti-HA, anti-GRASP, and DAPI suggests a Golgi apparatus location for both HA_3-TbFUT1-MYC_3 and HA_3-TbFUT1. The absence of anti-MYC (*A*) or anti-HA (*B-C*) staining under non-permissive conditions confirms the specificity of the labelling for the respective TbFUT1 fusion proteins. Scale bars: 3 µm.

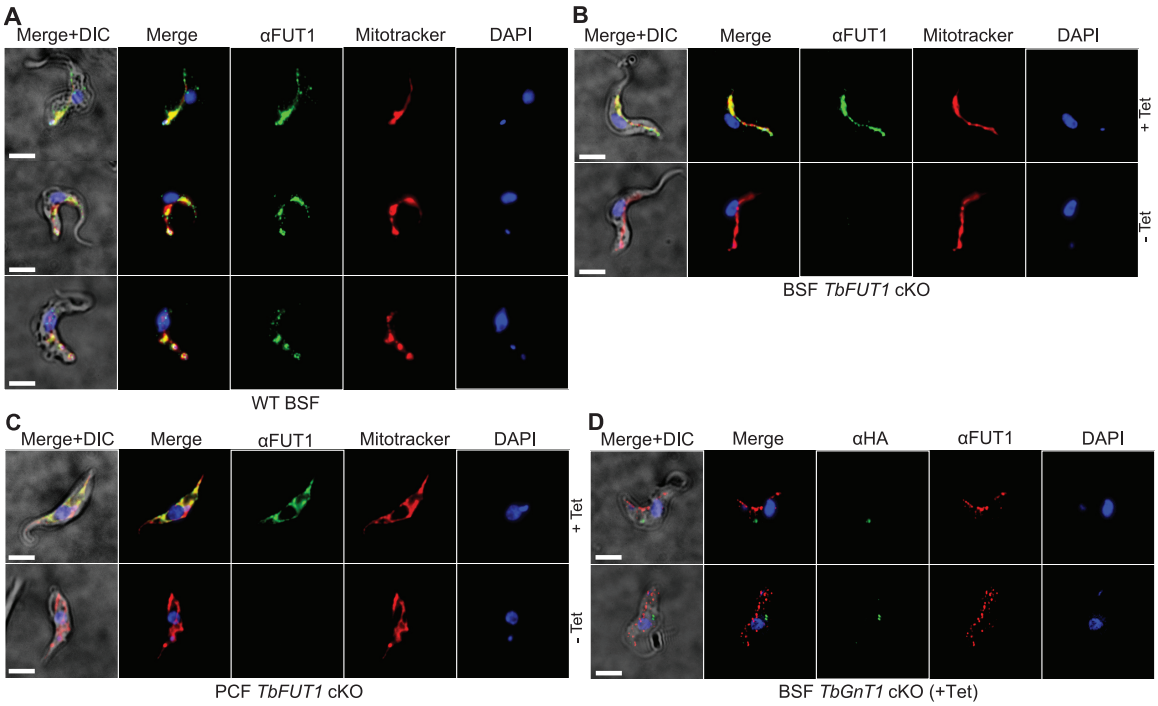

FIGURE 7. **Antibodies to the recombinant protein localize TbFUT1 to the mitochondrion**. *A*. IFA of wild type bloodstream form (BSF) trypanosomes after staining with affinity purified anti-TbFUT1 (αFUT1) MitoTracker™ and DAPI. Comparable patterns were observed for anti-TbFUT1 and MitoTracker™, suggesting TbFUT1 localizes to the mitochondrion. *B-C*. Bloodstream (*B*) and procyclic (*C*) form *TbFUT1* conditional null mutants were imaged under permissive (+Tet) and non-permissive (-Tet) conditions. In both cases the tetracycline-inducible TbFUT1 pattern is consistent with a mitochondrial localization. *D*. BSF trypanosomes induced to express a C-terminally tagged known Golgi glycosyltransferase (TbGnTI-HA_3) were imaged after staining with αFUT1, anti-HA and DAPI, as indicated. The merged images of two representative cells suggest no significant co-localization between native TbFUT1 and the Golgi-localized TbGnT1. Scale bars: 3 µm.

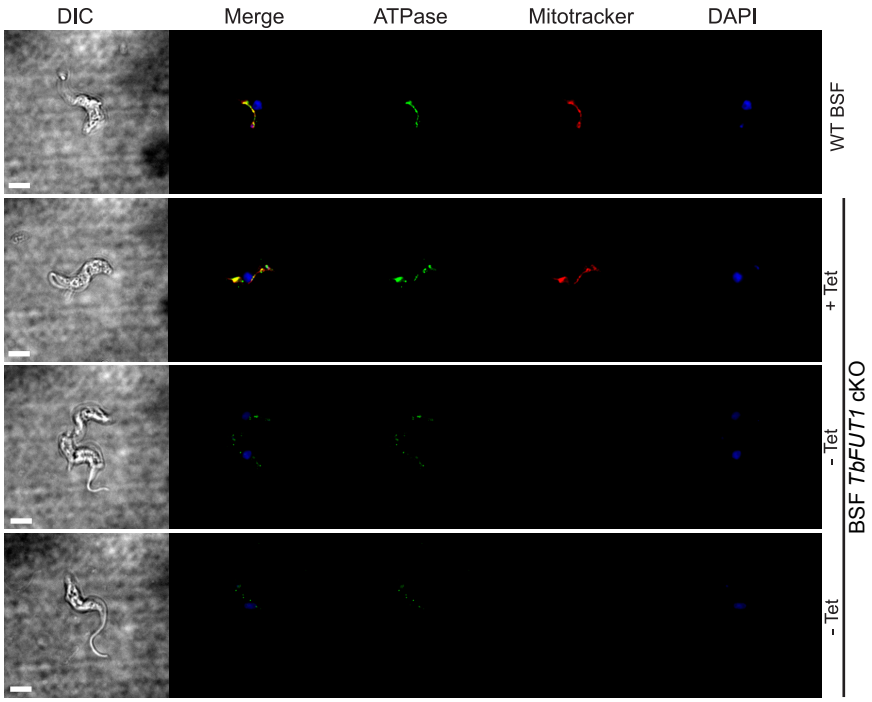

745

746 FIGURE 8. **Absence of TbFUT1 disturbs mitochondrial activity.** Bloodstream form (BSF)
747 wild type and *TbFUT1* cKO parasites were cultured for 5 days under permissive (+ Tet) and non-
748 permissive (- Tet) conditions, fixed and labelled with Mitotracker™ for mitochondrial potential
749 and with anti mitichondrial-ATPase antibody. In mutants grown in non-permissive conditions
750 (*lower panels*) both ATPase and Mitotracker staining are strongly reduced, suggesting reduced
751 mitochondrial functionality. Scale bar: 3 µm.

752